Journal of Undergraduate Chemistry Research, **2024**, 23 (3), 25

USING BIPHENYL TO PROBE THE EFFECT THAT ANNEALING HAS ON THE SURFACE MORPHOLOGY OF VAPOR DEPOSITED CHLOROALKANES ON Al_2O_3

Jessica M. Rosenfeld*, Reese M. Toepfer*, Alan O. Lopez*, Jesse C. Nieman*, Isabella Felix*, Jackson Zerwas* and A.M. Nishimura†

Department of Chemistry, Westmont College, Santa Barbara, CA 93108

Abstract

The conformer of biphenyl varies depending on the molecular environment. Biphenyl's dihedral angle is closely related to the energy of the singlet electronic state that can be detected by fluorescence spectroscopy. Therefore biphenyl is an ideal probe of the surface morphology of an adlayer upon which it is placed. With this in mind, the effect of annealing adlayers of a homologous series of chloroalkane, starting with 1-chloropropane through 1-chlorooctane, was investigated. Vapor deposition typically results in a highly amorphous adlayer. However annealing can have a huge ordering effect. 1-Chlorohexane, 1-chloroheptane and 1-chlorooctane showed that annealing does cause the adlayer to become highly organized presumably resulting in a parallel arrangement to each other that allows biphenyl in a planar conformer to deposit into the vacancies between molecules whereas 1-chloropropane, 1-chlorobutane and 1-chloropentane caused biphenyl to deposit on top in its normal twisted conformer. A tentative explanation for the latter result is that biphenyl did not fit within the structure, because of disorder in the adlayer. These results indicate biphenyl's potential use as a probe of surface ordering.

†Corresponding author: nishimu@westmont.edu *Undergraduate student researchers and co-authors

Keywords: 1-chloroalkanes, 1-chlorohexane, 1-chloroheptane, 1-chlorooctane, biphenyl, temperature programmed desorption, TPD, wavelength resolved TPD.

Submitted: June 12, 2024 Accepted: July 8, 2024 Published: July 29, 2024

Introduction

In the solid phase, biphenyl's dihedral angle between the two planar phenyl groups may vary.[1-3] In the gas phase, the dihedral angle is about 45°,[4] whereas in the crystalline state at room temperature, the two rings are in a double minimum potential and statistically centered.[2] The 45° dihedral angle that is observed in the gas phase is the result of the competition between the steric hindrance and repulsive forces of the ortho-hydrogens on one hand and the π-electrons that can delocalize with lower energy if the phenyl groups were co-planar.[3] The molecular fluorescence emission of biphenyl has been well documented.[5,6] The spectral profiles of several substituted biphenyls in which the biphenyl was in the planar and out-of-plane conformers have been examined.[7,8] The λ_{max} ~ 320 nm fluorescence has been assigned to the non-planar conformer of biphenyl and the λ_{max} ~ 340 nm fluorescence has been assigned to the planar conformer.[8,9] When vapor deposited on Al_2O_3 at 138 K, the amorphous planar conformer predominate and has a λ_{max} ~ 370 nm that has been attributed to the excimer.[8-11] More recently, the specific dihedral angles of biphenyl were correlated to the fluorescence spectrum.[12] For example, the 320 nm fluorescence has been attributed to the biphenyl conformer with a dihedral angle of 37º and the 340 nm fluorescence to a dihedral angle of 4º.[12]

By using light scattering, *n*-alkanes on graphite showed that hexane and longer alkanes gave rise to surface tension and surface energies that were higher than expected.[13-16] This was attributed to London dispersion forces between parallel molecules and the term, 'correlated molecular orientation', CMO, was ascribed.[13-16] By scanning tunneling microscopy, *n*-bromo- and *n*-chloroalkanes on graphite were studied that showed that the halogens were on the same side while the alkane groups crystallized side by side.[17,18]

In a previous study, biphenyl was used to probe the surface morphology created by these *n*-alkanes that had been deposited on Al_2O_3.[19] When the alkyl group was heptane and longer, the excimer of biphenyl was observed, instead of the twisted conformer observed with the shorter chain *n*-alkanes.[19] The tentative explanation was that due to CMO, these longer alkanes formed grooves into which biphenyl could land if it were in the planar conformer.[19] Reported in this paper are the results of additional studies in which biphenyl was used as a probe to determine the morphogy of the surface created by 1-chloroalkanes deposited as an underlayer. The dihedral angle of biphenyl was determined from the best fit line of the dihedral angle as a function of the wavelength of the fluorscence.[13] The surface morphology of the homologous series of 1-chloroalkanes can be inferred from the dihedral angles of biphenyl and allows an indirect alternative method to x-ray crystallography as shown in Scheme 1.

Experimental

Biphenyl and the chloroalkanes that were used in this sutdy were of the highest purity that were commercially available, > 99% (Sigma-Aldrich, St. Louis, MO). These compounds were placed in separate sample holders, outgassed and introduced into the ultra-high vacuum chamber with background base pressure of 1 x 10^{-9} torr. Deposition onto a single crystal of Al_2O_3 (0001) (Crystal Systems, Inc., Salem, MA) was accomplished from the vapor through variable leak valves. The substrate was suspended on the end of a liquid nitrogen cryostat via copper post on either

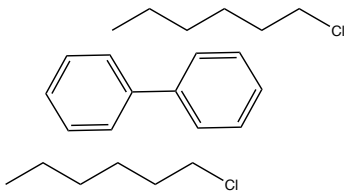

Scheme 1. Postulated molecular arrangement of biphenyl with 1-chlorohexane underlayer on Al_2O_3.

side of the Al_2O_3 with a sapphire spacer for electrical and thermal isolation. Resistive heating of the Al_2O_3 was done by sending current through a thin tantalum foil that was in thermal contact with the substrate. A type-K thermocouple that was also in thermal contact with the Al_2O_3 monitored the temperature.

Details of the experimental set up have been previously published[15] and a brief summary is given here. During the temperature programmed desorption, TPD, a LabVIEW (National Instruments, Austin, TX) program that was written in-house was used to take the fluorescence spectra from the Ocean Optics USB4000 spectrometer (Ocean Optics, Dunedin, FL) fluorescence spectra were acquired in real time every 300 ms. The program simultaneously monitors the surface temperature of the Al_2O_3 crystal, and via a PID (proportional-integral-derivative) feedback algorithm, linearly increments the temperature of the Al_2O_3 crystal in the TPD experiments. The program also scans the residual gases analyzer that detects the desorption of gases from the Al_2O_3. Manipulation of the array of spectra as a function of temperature by a MATLAB (Mathworks, Natick, MA) template yielded the wavelength resolved TPD's that are shown in the figures. To ensure a clean surface, the Al_2O_3 was heated to 300 K after each run.

The activation energy for desorption, E_a, was calculated by Redhead analysis in which a first-order desorption kinetics as described by King was assumed and is based on the mass spectral peak desorption temperature, T_p.[20-22] The uncertainties in the desorption temperatures and the propagated error in the activation energies were ± 2%.

The surface coverages, Θ, in monolayers (ML) were calculated by calibrating the integrated mass spectral peak areas to an optical interference experiment. The interference experiment yielded accurate rate of deposition with coverage error of ± 30%, and is described in detail elsewhere.[10]

For surface coverages in the multilayer regime, multidimensional nucleation and crystal growth is expected at the disorder-to-order transition. In order to model the disorder-to-order transition in biphenyl as a nucleation-crystallization process, the Johnson-Mehl-Avrami-Kolmogorov, JMAK, or simply, Avrami model was used.[23] In the simplest form, the Avrami equation is given by:

$$I(t) = e^{-kt^n}$$

where I(t) is the time dependent fluorescence intensity at the disorder-to-order transition that is converted to fraction of the disordered state at the transition, k is related to the rate with which crystallization occurs and is in part, a function of the density of nucleation sites, t is time in s, and n is the dimensionless Avrami exponent that yields the dimensionality of the nucleation-crystallization process.[23] The unit for k is the inverse of time raised to the n^{th} power. This expression was made to fit the wavelength-resolved TPD data at the disorder-to-order transition using algorithms provided by SciPy (an open-source Python library) and automated with Python (an open-source programming language, Python Software Foundation) in which the parameters were controlled by user interface.

In order to more accurately report the relative spectral intensities of overlapping peaks, spectral deconvolution was accomplished and reported. Codes were written in-house around Igor Pro 8.04. (WaveMetrics, Lake Oswego, OR) so that linear combinations of as many as five peaks of differing lineshape (gaussian or lorentzian), each representing different conformer of biphenyl, could be deconvoluted from the wavelength-resolved TPD data. The output of the program yielded the peak height, the standard deviation (full width at half of the maximum intensity, FWHM), and the x-position at the center of the peak.

Results and Discussion

Biphenyl

The peak desorption temperature, T_p, of neat biphenyl was 234 K. First-order desorption was assumed and the activation energy for desorption, E_a, was calculated to be 60.8 kJ/mol.[20-22] Upon deposition, excitation of neat biphenyl on the Al_2O_3 surface with a high-pressure Hg lamp centered at 250 nm caused the amorphous biphenyl to fluoresce with a λ_{max} of 320 nm. This fluorophore has been assigned to the twisted conformer of biphenyl with a dihedral angle of 37º.[12-13] As can be seen from Figure 1, when the surface temperature was linearly ramped, the adlayer underwent a disorder-to-order transition at 160 K, where λ_{max} red-shifted to 340 nm. This fluorophore has been assigned to the planar conformer of biphenyl with a dihedral angle of 4º.[12-13] The reduction in intensity to about 10% of the initial results from the ordered molecules becoming better energy carriers to the trap sites from which radiative relaxation occurred.[13]

1-Chlorohexane

Shown in Figure 2 is the wavelength-resolved TPD of biphenyl deposited on an underlayer of unannealed 1-chlorohexane. When Figure 2 is compared to Figure 1, it is apparent that the underlayer had almost *no* effect on the fluorescence spectrum of biphenyl. When the underlayer was annealed before adding biphenyl, either at 125 K for several seconds or at the deposition temperature (~ 120 K) for several minutes, the resulting wavelength resolved TPD is shown as Figure 3. The two peaks that are clearly resolved have λ_{max} ~ 355 and 370 nm. The 355 nm peak is attributed to the planar conformer with a dihedral angle of nearly 0º and

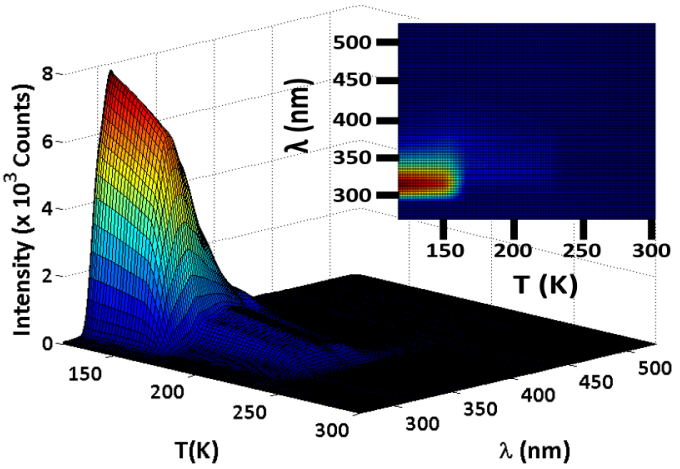

Figure 1. Wavelength-resolved TPD of multilayer biphenyl. $\Theta_{biphenyl}$ = 105 ML. Biphenyl deposited in the twisted conformation with λ_{max} ~ 320 nm that red-shifts to 340 nm subsequent to the disorder-to-order transition. Inset: top view.

the 370 nm is due to excimer.[8-11] The fluorescence blue-shifts to 340 nm subsequent to the disorder-to-order transition. When the fluorescence spectrum was deconvoluted, one additional peak was discovered at 390 nm. This has been tentatively attributed to the excited state trimer that has been reported in other molecules.[24] It is noteworthy that comparison of Figures 2 and 3 indicates that the fluorescence intensity of the 370 nm peak due to the biphenyl excimer (Fig. 3) is appoximately half that of the 320 nm peak when the underlayer is unannealed (Fig. 2). This gives support to the assignment that the 370 nm fluorescence is due to the excimer.

In order to acertain the optimum annealing temperature for the underlayer, the intensities of the excimer peak were monitored as a function of annealing temperature and the results are shown in Figure 4. For 1-chlorohexane, the annealing temperature was very nearly that of the deposition temperature so that after deposition, if the adlayer was simply kept at the deposition temperature, in time,

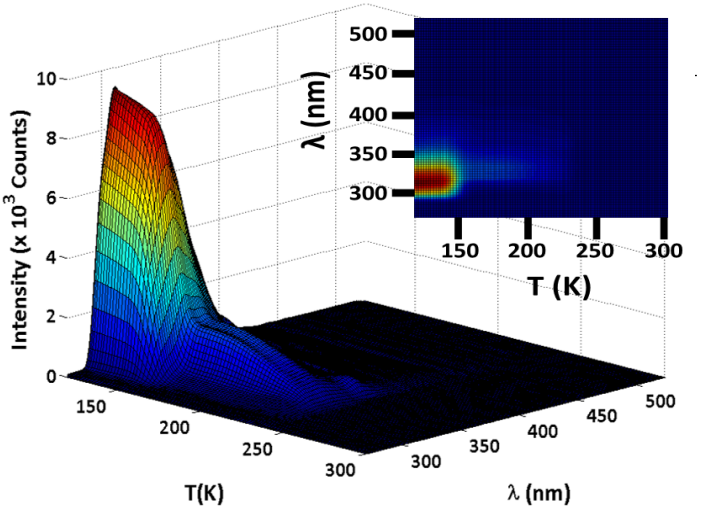

Figure 2. Wavelength-resolved TPD of a bilayer that consisted of an underlayer of unannealed 1-chlorohexane ($\Theta_{1\text{-chlorohexane}}$ = 183 ML) and biphenyl ($\Theta_{biphenyl}$ = 85 ML). The fluorescence at λ_{max} ~ 320 nm dominates at deposition that red-shifts to 340 nm subsequent to the disorder-to-order transition. Inset: top view.

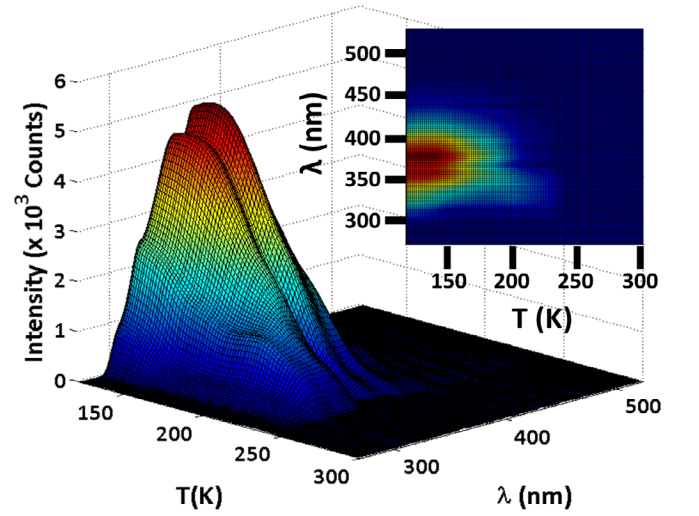

Figure 3. Wavelength-resolved TPD of a bilayer that consisted of an underlayer of 1-chlorohexane ($\Theta_{1\text{-chlorohexane}}$ = 100 ML) that had been annealed at 125 K for 1 minute. Subsequently, biphenyl wth $\Theta_{biphenyl}$ = 97 ML was deposited and the TPD experiment was done. The fluorescence at λ_{max} ~ 355 and 370 nm were dominant at deposition. A blue-shifted peak at 340 nm appears at the disorder-to-order transition. Inset: top view.

the intensity of the excimer peak increased with a concommitant decrease in the 320 nm peak intensity. For the sake of uniformity in the data, the underlayer was routinely annealed at 125 K.

Plotted in Figure 5 are the integrated intensities of the λ_{max} of the deconvoluted peaks at 320 and 340 nm in blue and orange, respectively as a function of the coverage of the annealed 1-chlorohexane underlayer in ML. The coverage of biphenyl was held constant at 105 ± 13 ML. What is evident is that at low coverages, the fluorescence was dominated by the 320 nm peak. This has been attributed to the twisted conformer of biphenyl that is observed in the gas phase.[12] From a previous study of the correlation of the dihedral angle with fluorescence, the dihedral angle of the twisted conformer is about 37º.[12] As shown in Figure 5, as the underlayer coverage was increased to ~ 70 ML, the intensities of the 320 and 340 nm peaks decreased with a concomittant increase in the 355, 370 and 390 nm fluorescence (Cf. Figure 6) until about 1000 ML at which coverage, intensity of the original 320 and 340 nm fluorescence peaks increased once again. Close examination of Figure

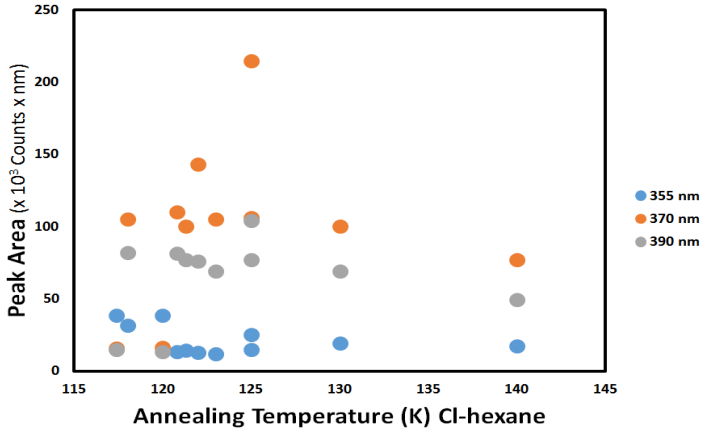

Figure 4. Plot of the deconvoluted peak areas of the 355 nm (blue), 370 nm (orange) and 390 nm (gray) as a function of annealing temperature of the 1-chlorohexane underlayer. Note that the x-axis is logarithmic. The $\Theta_{1\text{-chlorohexane}}$ = 101 ±10 ML and $\Theta_{biphenyl}$ = 105 ± 13 ML.

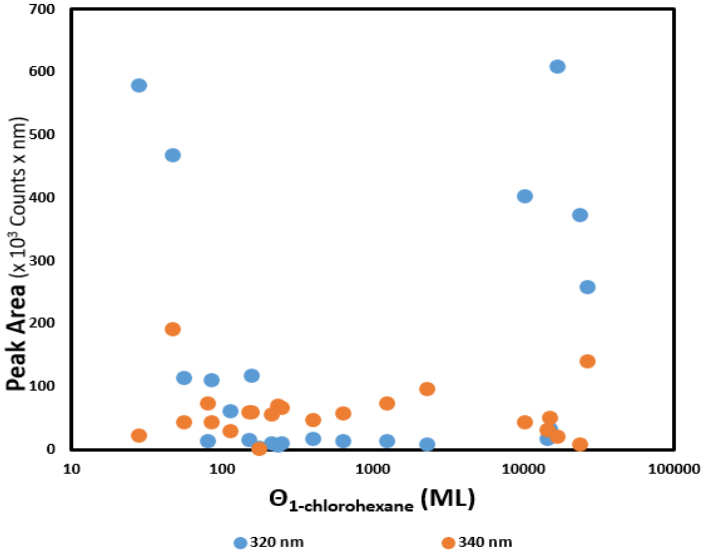

Figure 5. Plot of the deconvoluted peak areas of the 320 nm (blue) and 340 nm (orange) as a function of coverage of the 1-chlorohexane underlayer that had been annealed at 125 K. Note that the x-axis is logarithmic. The biphenyl coverage was held constant at 105 ± 13 ML.

6 shows that, in this window of underlayer coverages from 70 ML to 1000 ML, biphenyl exhibts the three fluorescence peaks at 355, 370 and 390 nm that have been attributed to the planar, excimer and trimer bipehnyl, respectively. When the coverage exceed 1000 ML, the data show that the underlayer was no longer aligned in such a way that adsorption binding sites were open for the biphenyl molecule to situate in a planar conformer.

It is also noteworthy that the integrated intensity of the most red-shifted 390 nm peak was about 40% of the integrated intensity of the 370 nm peak. Furthermore as noted, the 390 nm peak was only found upon deconvoluting the spectra and had been previously overlooked. The reason is due to the relatively broad linewidth of the 390 nm peak. Typical FWHM for the 370 and 390 nm peaks were 40 ± 0.5 nm and 31 ± 0.2 nm, respectively. (In comparision, typical FWHM for the 320 and 340 nm peaks were 8.5 ± 0.2 nm and 15 ± 0.2 nm, respectively). The unusually large linewidth is characteristic of excimers due to the inhomogeneous broadening that occurs because of the energetically wide distribution of excimers,[6] and of trimers, in this case. Hence, the red-shift, the relative intensity compared to the excimer, and the spectroscopically broad linewidth, give support to the tentative assignment that the 390 nm peak is due to the excited state trimer.

Avrami nucleation-crystallization model was used to determine the dimensionality of the crystallization as a function of coverage of 1-chlorohexane and is shown in Figure 7. The two dimensional nucleation-crystallization is nominal for such processes that occur on surfaces.[13] Note that at very high coverages (>1000 ML), the dimensionality of the nucleation-crystallization increases due to the disorder that can be assumed to prevail.

1-Chloroheptane

Figure 8 is the wavelength-resolved TPD of biphenyl that had been deposited on top of the 1-chloroheptane underlayer that had not been annealed. Comparison with Figure 1 shows that all 5 wavelengths are observed. Although not shown here, the optimum annealing temperature was determined by plotting the excimer intensity as a function of annealing temperature. When the underlayer was annealed at 130 K, the resulting wavelength-resolved TPD of biphenyl is shown in Figure 9. Notice that only the 355 and 370 nm peaks are immediately apparent and the 390 nm peak was only found by deconvolution. The plots corresponding to the 320 and 340 nm deconvoluted intensities as a function of annealed underlayer coverage are shown in Figure 10 and the deconvoluted integrated intensities of the 355, 370 and 390 nm peaks as a function of underlayer coverage that had been annealed at 130 K are shown in Figure 11.

As noted from Figure 10, the intensity of the 320 nm peak decreases with 1-chloroheptane coverages from about 1 to 100 ML, and then increases at coverges > 100 ML. This is mirrored in Figure 11, in which the window of 1-chloroheptane coverages from 1 to 100 ML exhibit increases in the 370 and 390 nm peaks. The 355 nm peak, with a dihedral angle of 0º, was very weak with 1-chloroheptane as the underlayer. The reason for this observation is that due to disorder in the underlayer at both the low coverages (< 1

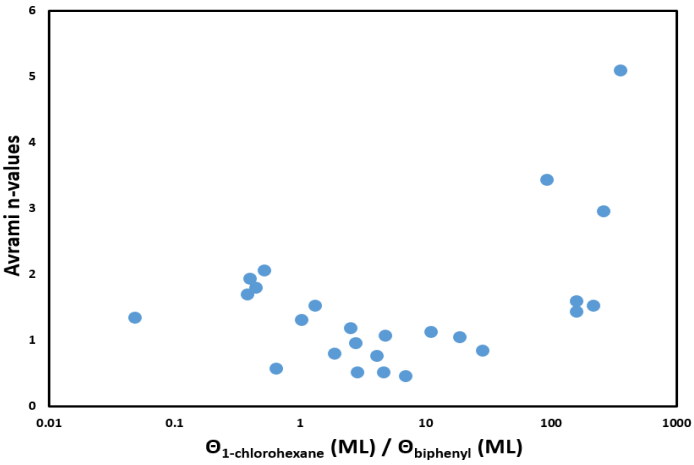

Figure 7. Plot of the Avrami n value as a function of the ratio of coverages for 1-chlorohexane (ML) and $\Theta_{biphenyl}$ (ML). The 1-chlorohexane underlayer that had been annealed at 125 K. Note that the x-axis is logarithmic. The biphenyl coverage was held constant at 105 ± 13 ML.

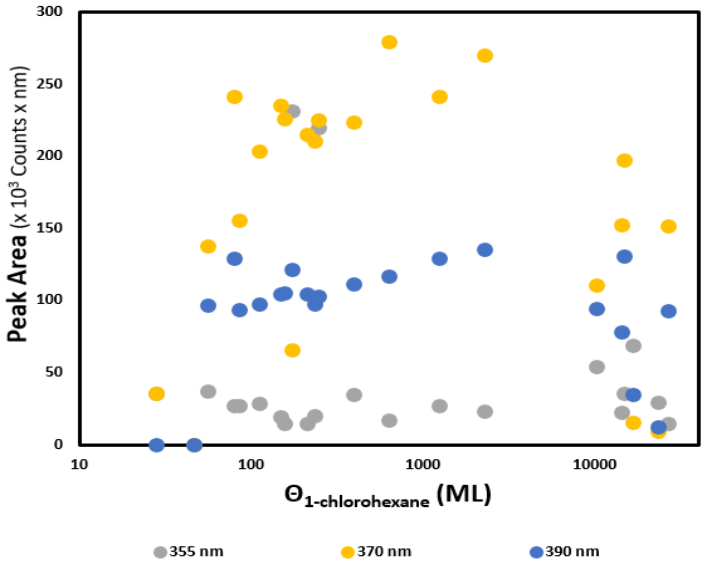

Figure 6. Plot of the deconvoluted peak areas of the 355 nm (gray), 370 nm (orange) and 390 nm (blue) as a function of coverage of the 1-chlorohexane underlayer that had been annealed at 125 K. Note that the x-axis is logarithmic. The biphenyl coverage was held constant at 105 ± 13 ML.

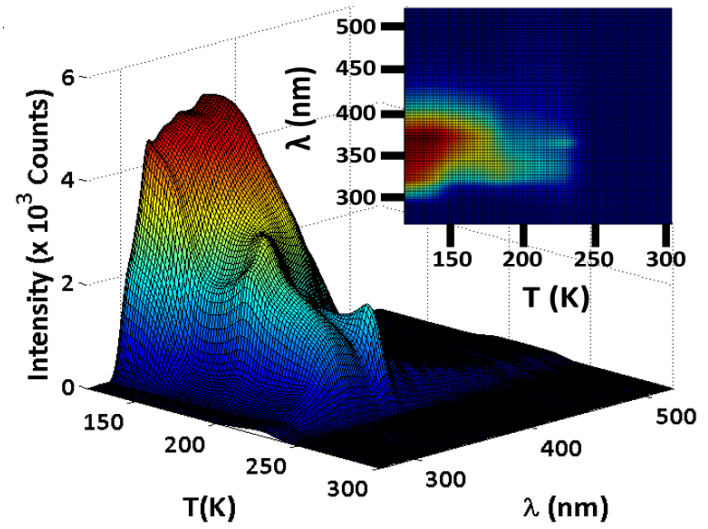

Figure 8. Wavelength-resolved TPD of a bilayer that consisted of an underlayer of unannealed 1-chloroheptane ($\Theta_{1\text{-chloroheptane}}$ = 18 ML) and biphenyl ($\Theta_{biphenyl}$ = 98 ML). The fluorescence from all species were observed at deposition, but then they all shifted to 340 nm subsequent to the disorder-to-order transition. Inset: top view.

ML) and high coverages (>100 ML), insufficient sites exist for biphenyl in the planar conformer to deposit in sufficient number to be detected. These findings are summarized in Table 1. In Figure 12, excimer intensities as a function of underlayer coverages are sumarized in a composite plot to facilitate comparision between the various underlayers.

1-Chlorooctane

The intensity of the biphenyl excimer was much lower with 1-chlorooctane as an underlayer compared to 1-chlorohexane and 1-chloroheptane, as noted by the lower intensities shown in the summary plot in Figure 12. The optimum window in which the biphenyl excimer exhibited enhanced intensity is estimated to be about 4- 800 ML of the 1-chlorooctane underlayer that had been annealed at 150 K.

1-Chloropropane, 1-Chlorobutane, 1-Chloropentane

Attempts were made to observe the biphenyl excimer for 1-chloropropane, 1-chlorobutane and 1-chloropentane underlayers. For these molecules, dispersion forces were insufficient to cause alignment of the alkyl group and CMO could not be achieved. Hence, biphenyl could not insert itself in the planar conformation in the absence of linear adsorption sites in the underlayer. The peak desorption temperatures and activation energies for desorption are shown in Table 1.

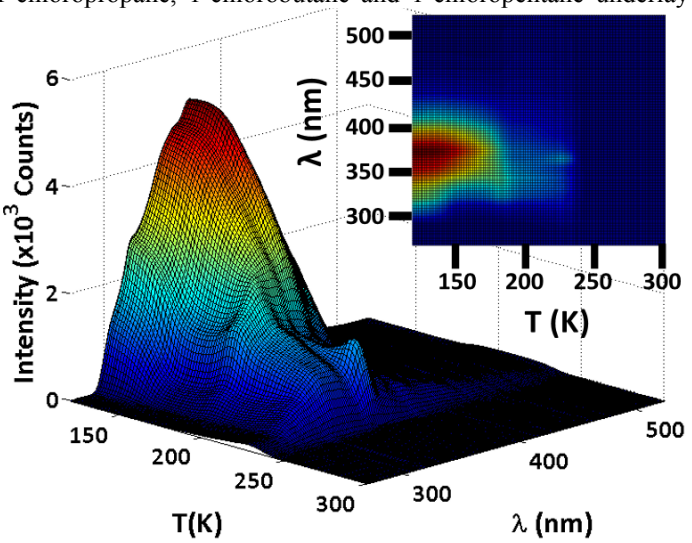

Figure 9. Wavelength-resolved TPD of a bilayer that consisted of an underlayer of 1-chloroheptane ($\Theta_{1\text{-chloroheptane}}$ = 19 ML) that had been annealed at 130 K and biphenyl ($\Theta_{biphenyl}$ = 91 ML). The fluorescence at λ_{max} ~ 355, 370 and 390 nm dominate at deposition. Inset: top view.

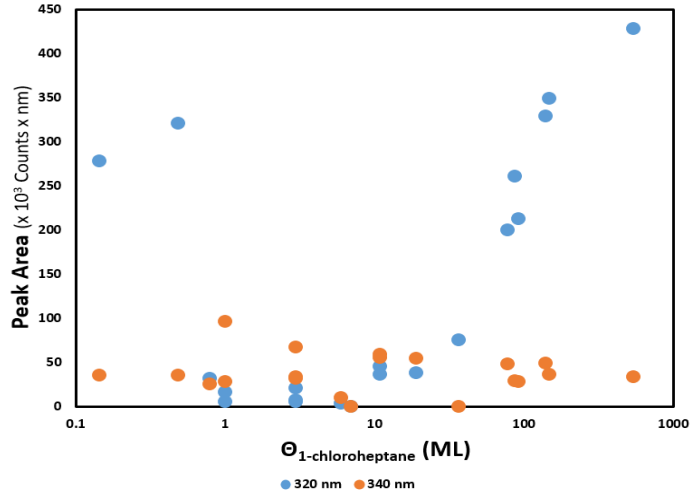

Figure 10. Plot of the deconvoluted peak areas of the 320 nm (blue) and 340 nm (orange) as a function of coverage of the annealed 1-chloroheptane underlayer. The biphenyl coverage was held constant at 99 ± 8 ML. Note that the x-axis is logarithmic.

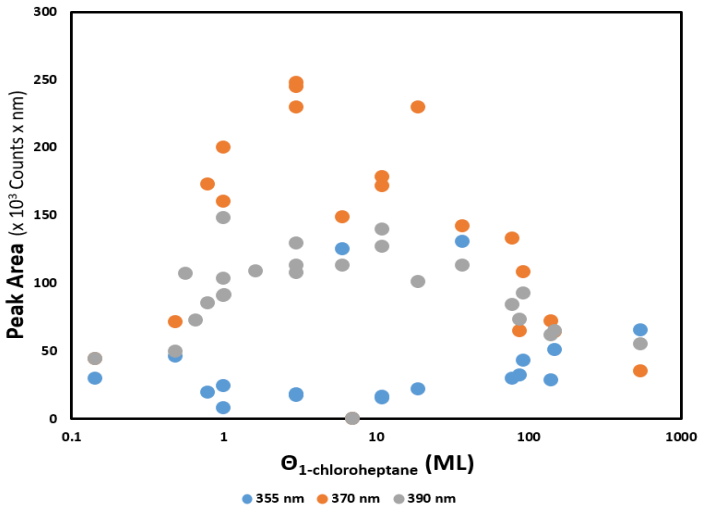

Figure 11. Plot of the of the 355 nm (blue), 370 nm (orange), and 390 nm (gray) deconvoluted peak areas as aa function of annealed underlayer coverage of 1-chloroheptane. The biphenyl coverage was held constant at 99 ± 8 ML. Note that the x-axis is logarithmic.

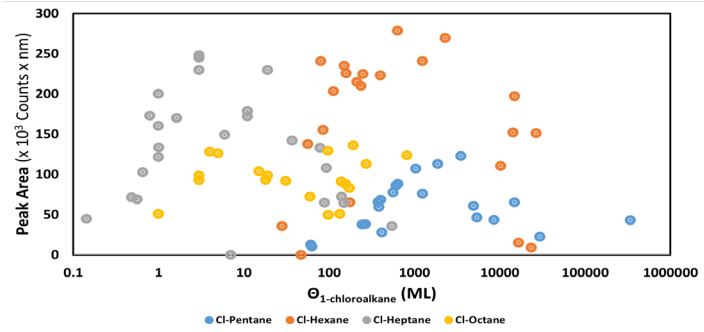

Figure 12. Composite plot of the deconvoluted peak areas of the 370 nm peak due to the biphenyl excimer for 1-chloropentane (blue) underlayer with $\Theta_{biphenyl}$ = 101 ± 10 ML. for 1-chlorohexane (orange) as shown in Fig. 6, for 1-chloroheptane (gray) as shown in Fig. 11, and 1-chlorooctane (yellow) underlayer with $\Theta_{biphenyl}$ =104 ± 18 ML. Note that the x-axis is logarithmic.

Table 1. Summary of the important data for all of the haloalkanes that were studied. The table includes the peak desorption temperatures, T_p (K), the activation energy of desorption, E_a (kJ/mol), whether or not excimer was observed with the unannealed underlayer, the annealing temperature (K), the range in the underlayer coverage that the excimer was observed (ML) and the n and k values in the Avrami equation that modeled the nucleation-crystallization.

Underlayer	T_p (K)	E_a (kJ/mol)	Excimer If Unannealed?	Anneal T for Max. $I_{excimer}$ (K)	Excimer Observed for $\Theta_{underlayer}$ (ML)	Avrami n	Avrami k
1-chloropropane	136 ± 7	35 ± 2	no			1.8 ± 0.11	0.17 ± 0.06
1-chlorobutane	157 ± 2	40 ± 1	no			1.7 ± 0.11	0.1 ± 0.14
1-chloropentane	162 ± 6	41.5 ± 1.5	no			3.1 ± 0.11	0.012 ± 0.005
1-chlorohexane	174 ± 4	41.5 ± 0.5	no	125	70-1000	1.7 ± 0.4	0.05 ± 0.04
1-chloroheptane	182 ± 4	47 ± 1	yes	130	1-100	1.5 ± 0.3	0.3 ± 0.14
1-chlorooctane	190 ± 5	48.5 ± 0.5	yes	150	4-820	1.6 ± 0.2	0.03 ± 0.02
1-bromohexane	172 ± 4	44 ± 1	no	155	4-12	2.1 ± 0.4	0.02 ± 0.02
2-chlorohexane	163 ± 3	42 ± 1	no			6 ± 3	0.003 ± 0.003
1,6-dichlorohexane	212± 3	55 ± 1	no			3.5±0.2	0.003±0.001
biphenyl (overlayer)	234 ± 3	60.8 ± 1				1.2±0.2	0.181±0.02

Other underlayers

1-Bromohexane

This compound was chosen to investigate the effect of a larger halogen on the underlayer's ability to form linear adsorption sites for biphenyl. 1-Bromohexane does form excimers but only in a very narrow range of coverages of about 4-12 ML.

2-Chlorohexane

The effect of asymmetry in the alkyl moiety was effective in removing its ability to form parallel structure for biphenyl in its planar conformation to insert into. Hence biphenyl excimer was not observed when 2-chlorohexane was the underlayer.

1,6-Dichlorohexane

Since the chlorine substituent is the attractive force that made the alkyl group align in parallel formation,[17,18] what would another chlorine on the tail end do? The biphenyl excimer did not form even when the underlayer was annealed to 170 K. The tentative explanation is that the two chlorines on each end cause the hexane groups to be closer together. This does not allow biphenyl sufficent room for insertion even in the planar conformation. The peak desorption temperatures and activation energies for desorption are given in Table 1.

Summary

Two factors, being able to determine the dihedral angle of biphenyl from the fluorescence λ_{max} and the sensitivity of the dihedral angle to molecular environment allow inferences to be made about the morphology of the underlayer. In this study, the parallel molecular arrangement of the alkyl group due to CMO can be induced by annealing the amorphous adlayer of chloroalkanes. From the graph (Figure 12) that summarizes the data, 1-chloroheptane required the lowest coverages to cause biphenyl to fit into adsorption sites in its planar conformer. 1-Chlorohexane required the next higher coverages. However the fact that the peak area was quite a bit lower meant that the number of adsorption sites was smaller than with 1-chloroheptane as the underlayer. 1-Chlorooctane came next, followed by 1-chloropentane. Shorter chloroalkanes than these did not show adsorption sites for biphenyl. The same was true for 2-chlorohexane and 1,6-dichlorohexane. 1-Bromohexane did allow excimers to form but not as much biphenyl adsorbed in the planar conformer.

Acknowledgement

The authors would like to thank the John Stauffer Charitable Trust for funding the student stipends for summer research. The authors would also like to thank Dr. Michael Everest of the Westmont College chemistry department for his help with Igor.

References

1. A. Almenningen, O. Bastiansen, L. Fernholt, B.N. Cyvin, S.J. Cyvin and S. Samdal. *J. Mol. Struct.*, **1985**, 128, 59-76.
2. G.P. Charbonneau and Y. Delugeard. *Acta Crystallographica B*, **1976**, 32, 1420-1423.
3. G. Friedrich. *J. Phys. Chem. A*, **2002**, 106, 3823-3827.
4. K. Ravindra, R. Sokhi and R. Van Grieken. *Atmospheric Environment*, **2008**, 42, 2895-2921.
5. I.B. Berlman. Handbook of Fluorescence Spectra of Aromatic Molecules, 2nd edition, Academic Press, New York, NY (1971) pp.176-177,330.
6. J.B. Birks. Photophysics of Aromatic Molecules, John Wiley & Sons Ltd., New York, NY (**1970**), pp. 301-370.
7. Marissa K. Condie, Zackery E. Moreau and A.M. Nishimura, *JUCR.*, **2019**, 18, 15-18.
8. B.D. Fonda, M.K. Condi, Z.E. Moreau, Z.I. Shih, B. Dionisio, A. Fitts, L. Foltz, K. Nili and A.M. Nishimura. *J. Phys. Chem. C*., **2019**, 123, 26185-26190.
9. M.K. Condie, C. Kim, Z.E. Moreau, B. Dionisio, K. Nili, J. Francis, C. Tran, S. Nakaoka and A.M. Nishimura. *JUCR*, **2020**, 19, 14-17
10. M.K. Condie, B.D. Fonda, Z.E. Moreau and A.M. Nishimura. *Thin Solid Films*, **2020**, 697, 137823.
11. K. Sasaki, M. Nagasak and Y. Kuroda, *Chem. Commun*. **2001,** 2630-2631.
12. N.M. Bond and A.M. Nishimura, *JUCR,* **2022**,21, 84-92.
13. Frederick M. Fowkes, *J. Phys. Chem*., **1980**, 84, 510-512.
14. M. Anwar, F. Turci and T. Schilling, *J. Chem. Phys*. **2013**, 139, 214904.
15. T. Arnold, C.C. Dong, R.K. Thomas, M.A. Castro, A. Perdigon, S.M. Clarke and A. Inaba, *Phys. Chem. Chem. Phys*., **2002**, 4, 3430-3435.
16. T.Arnold, R.K. Thomas, M.A. Castro, S.M. Clarke, L. Messe and A. Inaba, *Phys. Chem. Chem. Phys.*, **2002**, 4, 345-351.
17. G.M. Florio, T.L. Werblowsky, B. Ilan, T. Muller, B.J. Berne and G.W. Flynn, *J. Phys. Chem*., **2008**, 112, 18067-18075.
18. T. Muller, T.L. Werblowsky, F.M. Florio and G.W. Flynn, *PNAS*, **2005**, 102, 5315-5322.
19. I.Z. Song, S.T. Watanabe and A.M. Nishimura. *JUCR*, **2023**, 22, 66-68.
20. P.A. Redhead. *Vacuum*, **1962**, 12, 203-211.
21. F.M. Lord and J.S. Kittelberger. *Surf. Sci.*, **1974**, 43, 173-182.
22. D.A. King. *Surf. Sci.*, **1975**, 47, 384-402.
23. M. Avrami, *J. Chem. Phys*. **1939**, 7, 1103-1112; **1940**, 8, 212-224.
24. M. Fujitsuka, O. Ito and H. Konami, *Bul. Chem. Soc. Jpn.* **2001**, 74, 1823-1829.